PAPER VII

Amplifier Linearisation Using RF Feedback and Feedforward Techniques

Michael Faulkner, Mark A.Briffa
Mobile Communications and Signal Processing Group,
Victoria University of Technology
Box 14428 MMC, Melbourne 3000, AUSTRALIA

Abstract -- **The performance of feedback as a distortion reduction technique is highly dependent on the integrity of the feedback path. Any error or noise generated in this path is directly reflected into the output of the amplifier. Cartesian feedback requires a demodulator in the feedback loop and this is a potential source of linear errors, nonlinear errors, and noise. RF feedback with cartesian compensation is proposed as a technique for overcoming these problems. In addition the RF nature of the input, feedback and error signals makes the system suitable for incorporating into a feedforward system to further improve the linearisation capability. Design equations and simulation results are given for such a system.**

I. INTRODUCTION

Cartesian feedback is a common technique for linearising RF power amplifiers which carry signals having amplitude variations. AM to AM and AM to PM amplifier errors are approximately reduced by the loop gain. Improvements of more than 30dB in out of band distortion spectra are possible using this technique [1]. The performance for a given amplifier is generally limited by the integrity of the feedback demodulator circuit and the delay around the loop. The former can lead to the presence of carrier leak, noise, linear distortion and nonlinear distortion in the output signal and the latter limits the loop gain-bandwidth product. This paper describes an RF feedback technique that is much less sensitive to error sources in the signal processing elements and can also be combined easily into an integrated feedforward/feedback system for improved linearisation performance. The next section describes the cartesian feedback system and its performance with respect to variations in the signal processing components. The new scheme, RF feedback with cartesian compensation, is introduced in section 3. Section 4 shows how the new scheme can be incorporated into a feedforward system and how the additional linearisation capability can be used to increase the bandwidth of the feedback section. Expressions for the system performance are derived.

II. CARTESIAN FEEDBACK

Figure 1 shows a simplified block diagram of a cartesian feedback system suitable for analysis. Bold lines represent the I and Q complex baseband signals. d_m represents the noise and distortion introduced by the forward path components, and d_d the noise and distortion of the feedback components. The amplifier distortion is d_a.and -wta+δ represents the overall phase rotation around the loop caused by the rf components and the loop delay, τ_a respectively. δ is normally adjusted to set the loop phase rotation to 0 degrees by offseting the phase of the LO drive signals between the modulator and demodulator. The output signal is given by:

$$y = x\frac{(((x - d_d)G + d_m)\, g e^{j(-\omega\tau_a + \delta)}) + d_a}{1 + HgG\, e^{j(-\omega\tau_a + \delta)}} \qquad (1)$$

where

$$d_m(f) = n_m + p_m + v_m f^* + a_m(f)$$
$$d_d(Hy) = n_d + p_d + v_d Hy^* + a_d(Hy)$$
$$d_a(r) = g_a(r)$$

The non-linear distortion terms am(•), ad(•), and ga(•) are non-linear functions of the applied signals, f, Hy, r, into the modulator, demodulator and the non-linear amplifier. Linear errors in the modulator and demodulator circuits generate carrier leak, p_m, and dc offset, p_d as well counter rotating signals with gains of $v_{m,d}$ caused by differential gain and phase misalignments of the quadrature circuits. G represents the gain of the baseband circuits and the loop filters and H is the attenuation in the feedback required to set the system gain and determine the signal level into the demodulator circuit. HgG = L is the loop gain, and when this is large

$$\frac{e^{j(-\omega\tau_a + \delta)}}{1 + HgG\, e^{j(-\omega\tau_a + \delta)}} \approx \frac{1}{L}$$

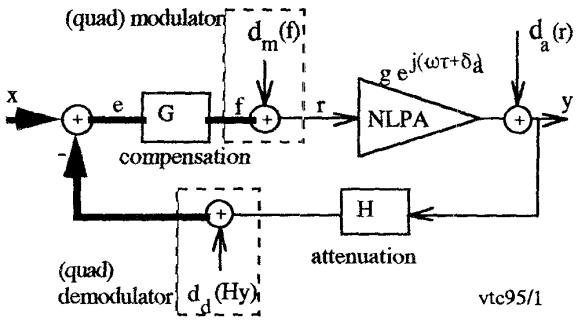

Figure 1 Cartesian feedback model with error sources. Baseband signals are in bold.

A. Quadrature Modulator and Demodulator distortion.

Linear distortions in these circuits cannot be eliminated by reducing signal level. The relative dc offsets (carrier leak) get worse as the signal levels are reduced and additional dc nulling circuits are often necessary. Other linear distortions introduced by the quadrature modulator such as differential

0-7803-2742-X/95 $4.00 © 1995 IEEE

gain and phase misalignments produce a counter rotating signal y* of amplitude v, where v is given by [2]

$$v \approx 0.5\sqrt{\delta_k^2 + \phi^2} \quad \exp\left(j \tan^{-1} \frac{\phi}{\delta_k}\right) \qquad (2)$$

where δ_k is the gain difference between the I and Q channels and ϕ is the phase difference from $\pi/2$.

Non-linear distortions in the modulator / demodulator mixers can be modelled using a 3rd order model for each mixer. Considering the demodulator, the input in cartesian form $Hy = H(y_{real} + j\, y_{im})$ and the distortion component becomes

$$\begin{aligned} a_d(Hy) &= a_3 H^3((y_{real})^3 + j(y_{im})^3) \\ &= a_3 H^3((y + y^*)^3 + (y - y^*)^3)/8 \\ &= a_3 H^3(2y^3 + 6|y|^2 y^*)/8 \end{aligned} \qquad (3)$$

where H is assumed to be real (normally an attenuator), and the small distortion coefficient a_3 is also real and assumed the same for both mixers. y^* is the conjugate of y.

B. Distortion in the feedback path.

Considering only the demodulator distortions in (1) and substituting y_d as the desired output signal .

$$y = (x - d_d(Hy))\frac{gG\, e^{j(-\omega\tau_a+\delta)}}{1+HgG\, e^{j(-\omega\tau_a+\delta)}} = y_d - d_d(Hy)/H \qquad (4)$$

The above equation can be solved iteratively for y provided $d_d(Hy)/H$ is small. After one iteration:

$$\begin{aligned} y &\approx y_d - d_d(Hy_d)/H \\ &\approx y_d - a_3H^2(2y_d^3 + 6|y_d|^2 y_d^*)/8 + v y_d^* + (n_d+p_d)/H \end{aligned} \qquad (5)$$

The spectrum of the counter rotating vector y_d^* is an inverted version of y_d and represents the unwanted sideband in a single sideband system.. There is no spectral expansion if the transmitted signal is single channel, but this could provide a problem for multi-channel signals or when baseband frequency correction is used for frequency drift or doppler compensation. The distortion terms are proportional to the cube of the amplitude and consists of a counter rotating term, $|y_d|^2 y_d^*$ and a forward rotating term, y_d^3, that has 3 times the deviation of the desired signal. Both terms cause spectral expansion. The distortion is proportional to H^2, but reducing H also increases the gain which causes the effect of noise and carrier leak (n_d + p_d) to increase in the output. A detailed analysis of the trade-off between noise and distortion is given in [3].

C. Distortion in the forward path.

A similar process is used to derive the modulator distortions. Two output expressions are obtained from Figure 1 and (1):

$$y = g\, e^{j(-\omega\tau_a + \delta)}(f + d_m(f)) \text{ and} \qquad (6a)$$

$$y = y_d + d_m(f)\frac{g\, e^{j(-\omega\tau_a + \delta)}}{1 + HgG\, e^{j(-\omega\tau_a + \delta)}} \qquad (6b)$$

eliminating y and solving for f using iteration, assuming $d_m(f)$ is small gives $f \approx y_d/ge^{j(-\omega\tau_a+\delta)}$. Substituting for f

$$y = y_d + d_m(y_d/ge^{j(-\omega\tau_a+\delta)})\; ge^{j(-\omega\tau_a+\delta)}/L \qquad (7)$$

Substituting for $d_m(\cdot)$

$$\begin{aligned} y = y_d &+ (1/L)[(n_m+p_m)ge^{j(-\omega\tau_a+\delta)} + v_m y_d^* e^{j2(\omega\tau_a-\delta)} \\ &+ (a_3 8g^2)(2e^{j2(-\omega\tau_a+\delta)} y_d^3 + 6\, e^{j2(\omega\tau_a-\delta)}|y_d|^2 y_d^*)] \end{aligned} \qquad (8)$$

The linear distortions are reduced by the loop gain. Carrier leak and noise at the modulator (n_m + p_m) are reduced by the loop gain when measured at the output. Non-linear distortion is reduced by the loop gain, and the amplifier gain squared. Increasing g reduces the signals in the mixers and degrades the relative carrier leak and out of band noise performance.

A similar analysis shows that the amplifier distortion, which is a function of the input magnitude, $d_a = g_a(r)$ is reduced by the loop gain.

$$y \approx y_d + g_a(y_d/g)/L\, e^{j(-\omega\tau_a+\delta)} \qquad (9)$$

In conclusion the forward path distortions d_m and d_a are both reduced by the loop gain, while any distortions added to the feedback path show up at the output as if they were another input signal. The performance of cartesian feedback systems is particularly sensitive to the integrity of the feedback circuits.

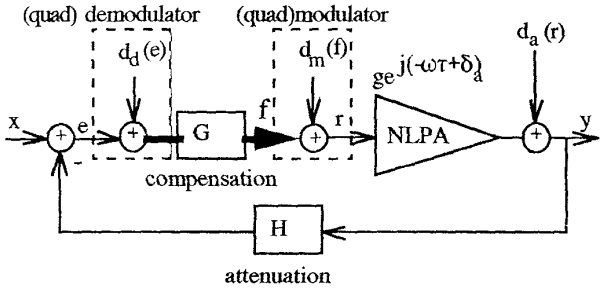

Figure 2 RF feedback with cartesian compensation. Bold lines represent baseband I and Q signals.

III. RF FEEDBACK

In this section we propose the use of RF feedback as a means of eliminating the processing elements in the feedback path. The signal processing elements are removed from the feedback loop as shown in Figure 2. The compensation circuits are difficult to implement at RF, because of the narrow bandwidths involved and the need for tuning over a reasonable range. The compensation circuits therefore remain in baseband and so the modulator and demodulator circuits are still required. They are however in the forward path and so a greater amount of demodulator error can be tolerated. Signal levels for the demodulator can be kept considerably higher further reducing susceptibility to dc offsets (carrier leak) and noise. DC correction circuits [4] are now no longer needed and the unwanted spectrally inverted products caused by

differential gain and phase misalignments are heavily attenuated. Multi-channel signals as well as modulations with frequency offsets are now possible.

The disadvantage is that the output signal can only be as good as the RF input signal, and so many of the problems move to the input RF modulator. However, other quadrature modulator structures are now possible (eg DSP quadmod or DDS waveform generation) which eliminate many of the problems. There is still a need for an RF phase adjuster, δ, as in cartesian feedback.

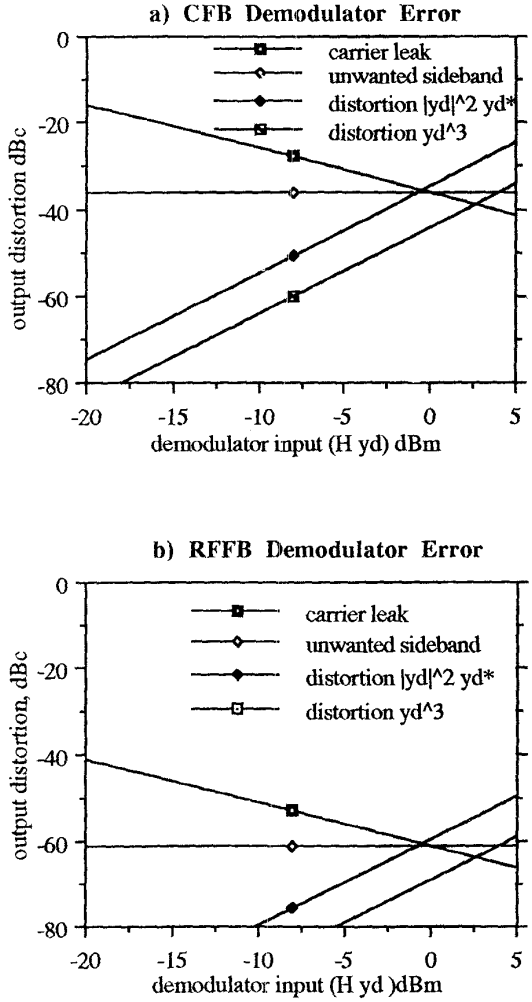

Figure 3 Relative distortion caused by quadrature demodulators in feedback systems. a) cartesian feedback, and b) RF feedback.

A. Design Example.

This example compares the output distortions produced by the demodulator of a Cartesian feedback system with the proposed RF feedback system. Both have a loop gain of 25dB. A single sideband tone (constant amplitude rotating phasor) is the input signal. The quadrature demodulator has the following specifications: conversion gain = - 8dB, amplitude misalignment = 1.7%, phase misalignment= 0.026 radians (1.5 degrees), dc offset, p_d = 1mV (-44dBm), and input 3rd order intercept, IM_3 = 16dBm.

From (2), the suppression of the unwanted sideband,v, is -36dB (0.0158). The distortion coefficient, a_3, of the mixer can be calculated from the IM_3 specification since the signal and 3rd order distortion components are equal at this point

$$IM_3 = a_3 (IM_3)^3 \qquad (10)$$

giving a_3 = 0.025. Substituting into (5) for cartesian feedback, and noting the 8dB (0.4) conversion loss applies to the desired and distorted signals only (not the dc offset or noise).

$$y \approx y_d+0.025H^2(2y_d^3+6|y_d|^2y_d^*)/8+0.016yd^* +(n_d+p_d)/(0.4\,H) \qquad (11)$$

Figure 3a plots carrier leak, unwanted sideband and the two distortion products against Hy_d the input to the demodulator.

The demodulator input should be lower than -13.5dBm to meet a 60dB output distortion criteria. At this level the carrier leak is nearly -20dBc. Special circuits are needed to reduce the carrier leak and unwanted sidebands. The effect of moving the demodulator to the forward path is to reduce all distortion components by the loop gain. The equation for the output distortions for an RF feedback system can be obtained by appropriately modifying (7)

$$y = y_d+[(n_d+p_d)Gg/0.4+0.016y_d^*+(0.025/8G^2g^2) (2y_d^3+6|y_d|^2y_d^*)]1/L \qquad (12)$$

Figure 3b shows the effect of a 25dB loop gain which allows the demodulator to be run at a higher level. An input of -0.5dBm into the demodulator will enable all distortion products (non-linear and linear) to be held below -60dBc, a significant improvement.

IV. FEEDBACK - FEEDFORWARD

Traditional feedforward systems have a signal cancellation loop that subtracts the distorted amplifier output from the amplifier, the resulting error signal substantially contains only the distortion products. This error signal is then amplified to the desired level and subtracted from the main signal to remove the distortion products from the main output signal [5].

The error signal, e, from the RF feedback loop (figure 2) represents the difference between the desired input signal and an attenuated version of the amplifier output. It is not effected by distortions in the feedback path and so could be used as the error output signal for a feedforward system. In addition the error signal is at RF, so modulation of the signal prior to feeding into the auxiliary amplifier is not needed; this reduces the potential for distortions in this loop.

Figure 4 shows a feed-forward system using an RF feedback loop as the first signal cancellation loop. The coefficient g_2 is adjusted to give the correct amplitude and phase for the feedforward cancellation loop.

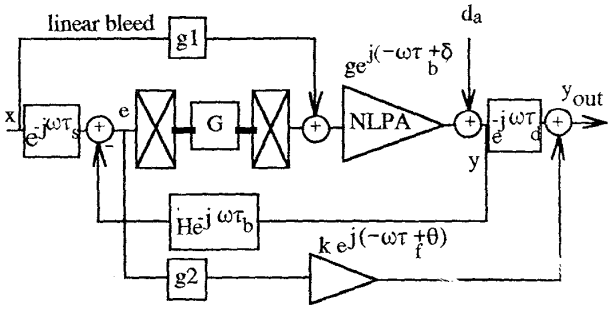

Figure 4 Analytical model of Feedback/feedforward. g_1 controls the signal cancellation loop and g_2 the error cancellation loop

The feedback / feedforward system has a number of advantages, the additional linearisation provided by the feedforward system allows the loop gain of the RF feedback system to be reduced and this can be traded for other features such as a greater tolerance in the adjustment of the loop phase compensation circuit (δ) or increased bandwidth. Also the loop gain of the feedback system reduces the need for critical adjustment in the two feedforward loops.

Table 1 Simulation Conditions

Parameter	Value
G	p/(s+p)
pole frequency, p	100kHz
τ_b , τ_f	0
τ_a	64ns
H, k, g_1	1
g_2	0.8 exp(j 10 π / 180)
δ, θ	0
amplifier, g	$10.0(1.867-(1.3557+j0.4577)\lvert r\rvert^2 + (0.4509+j0.1553)\lvert r\rvert^4)r$

In feedforward systems it is important to keep the auxiliary amplifier as small as possible in order to maintain reasonable efficiency. The signal in the auxiliary amplifier should be limited to distortion products only. Unfortunately the error signal from a feedback system still has a significant signal component (Figure 5). The bleed coefficient g_1 is used to reduce this signal component by bleeding some of the applied input signal directly into the input of the NLPA. This relieves the feedback error circuit from providing the main drive signal to the amplifier. The error signal should now only contain the distortion component. A simulation of the effect for a two-tone input signal is shown in Figure 5. The dotted trace is for reference purposes and shows the open-loop amplifier response, Hy, at the input to the subtractor (ie no distortion correction). The next trace shows the error signal, e, when feedback is applied (20dB loop gain). Both the distortion and the desired signal components are reduced but the error signal is still dominated by the desired signal. With the signal bleed switched on (g_1 activated) the desired signal components are reduced below the distortion components. Simulation details are given in Table 1.

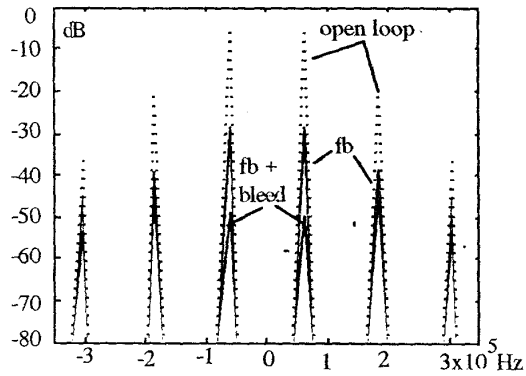

Figure 5. The error signal, e, from a two-tone test of a non-linear amplifier. The effect of the bleed coefficient g_1 is to reduce the signal components by a further 10 to 20dB.

A. Sensitivity Analysis.

The equation of the output is given by:

$$y_{out}= y\,e^{-j\omega\tau_d} + e\,g_2\,k\,e^{j(-\omega\tau_f+\theta)} \quad (13)$$

$$y_{out}=\{xe^{-j\omega\tau_s}(1+(g_1/G)e^{j\omega\tau_s})gGe^{j(-\omega(\tau_a+\tau_d)+\delta)}+d_ae^{-j\omega\tau_d} +xe^{-j\omega\tau_s}(kg_2e^{j(-\omega\tau_f+\theta)}-g_1g_2kHge^{j(\omega(\tau_s-\tau_a-\tau_b)+\delta+\theta)}) -d_aHkg_2e^{j(-\omega(\tau_b+\tau_f)+\theta)}\}\frac{1}{1+HgGe^{j(-\omega(\tau_a+\tau_b)+\delta)}} \quad (14)$$

The conditions for distortion cancellation are:

$$\tau_b+\tau_f=\tau_d \quad \text{and} \quad H\,k\,g_2\,e^{j(\theta)}=1 \quad (15)$$

Minimum forward loop error signal, e, requires:

$$\tau_b+\tau_a=\tau_s \quad \text{and} \quad H\,g\,g_1\,e^{j(\delta)}=1 \quad (16)$$

The coefficients g_1 and g_2 can be adjusted to fulfil these conditions. Their adjustment should not be as critical as in a standard feedforward system because the effect of any error is reduced by the loop gain of the feedback section. In addition, the delay match shouldn't be as critical either since this system is not suitable for wideband signals.

Figure 6 shows the effect of changing the tone separation on the error signal power. With no bleed signal through g_1, the error power is dominated by the signal component. The error power rises with frequency as the loop gain starts to drop (the pole frequency is at 100KHz). When the bleed coefficient is activated there is an approximate reduction in error power of about 10dB, as the signal component is further reduced. The error power for signal bandwidths up to 100KHz is less than 28dB down on the input power. Delay matching is only required for frequencies above 150kHz.

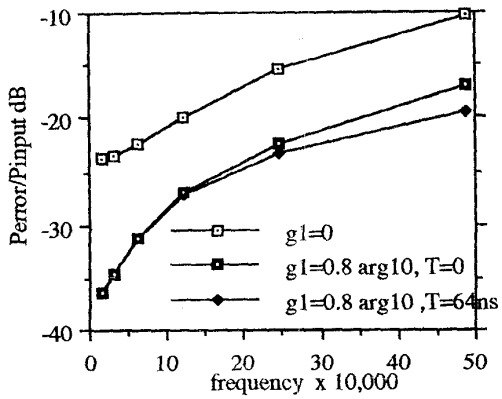

Figure 6 The power of the error signal for a two-tone input signal with various bleed path conditions set by g_1. The tone frequency is measured from band centre.

Figure 7 plots distortion improvement against input frequency for the feedback (fb), and the combined feedback / feedforward (fb_ff) cases. The effect of adjustment errors of 10% and 3% in the g_2 coefficient are shown. An additional large delay error of 32ns (equation 15) causes the curves to increase with frequency, otherwise they would have remained parallel with the fb curve. Clearly there is good performance out to 250KHz (500kHz two sided bandwidth) with a reasonable tolerance on the adjustment of g_2.

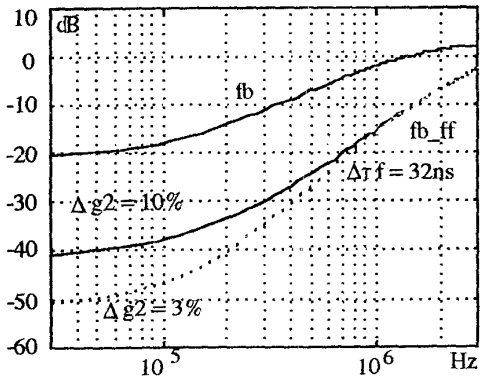

Figure 7 Distortion gain vs bandwidth (from bandcentre). Upper curve feedback (fb) only, middle and lower curves, feedback / feedforward (fb_ff) with coefficient adjustment error as marked.

V. CONCLUSION

Two new linearisation schemes have been proposed. The first, RF feedback with cartesian compensation, removes all processing from the feedback path, and so eliminates potential causes of noise and distortion that can degrade the system performance. In common with cartesian feedback the compensation circuits still remain in baseband and this facilitates tuning, easy adjustment and low cost design. The system requires an LO and a RF, rather than baseband, input signal which might be considered a drawback for some applications. However, it does not require special compensating circuits for the linear distortions of the quadrature demodulator (eg dc offset removal) and should have a good efficiency with a low noise floor.

The second linearisation scheme incorporates a feedforward loop into the RF feedback system. The main advantage is that the adjustment sensitivities of the signal and error cancellation loops are reduced by the loop gain and, depending on the application, the coefficients g_1 and g_2 could be held constant (ie no adaptation necessary). For the system described a reduction in distortion of over 32dB was possible for signals with distortion products of up to 500kHz (2 x 250kHz) bandwidth. However the bandwidth of the original signal should be limited to 200kHz (2 x 100kHz) because of the need for a low error signal, e, into the auxiliary amplifier. Further increase in bandwidth requires a reduction in loop delay, τ_a.

REFERENCES

1. Briffa, A. and M. Faulkner, *Gain and phase margins in cartesian feedback.* submitted to Journal of Electrical and Electronic Engineers Australia, 1994..

2. Faulkner, M., T. Mattsson, and W. Yates, *Automatic adjustment of quadrature modulators.* IEE Electronics Letters, 1991. 27(3): p. 214-216.

3. Johansson, M., *Linearisation of RF power amplifiers using cartesian feedback*, 1991, *Teknisk Licentiat*, Lund University, Sweden.

4. Bateman, A., D.M. Haines, and R.J. Wilkinson, *Direct conversion linear transceiver design*, in *Proceedings of the 5th International Conference on Mobile Radio and Personal Communication.* 1989. Warwick, U.K.: p. 53-56.

5. Stewart, R.D. and F.F. Tusubira, *Feedforward linearisation of 950MHz amplifiers.* IEE Proceedings, 1988. 135(5): p. 347-349.

PAPER IX

PERFORMANCE OF AUTOMATIC PHASE ADJUSTMENT USING SUPPLY CURRENT MINIMISATION IN A RF FEEDBACK LINEARISER

M. Faulkner, D. Contos and M. Briffa
Department of Electrical and Electronic Engineering,
Victoria University of Technology, Footscray Campus
PO Box 14428 MCMC, Melbourne 8001, AUSTRALIA
e-mail: mf@cabsav.vut.edu.au

ABSTRACT

Amplifier linearisation schemes based on feedback (e.g. cartesian feedback) require a phase correction circuit to stop instability and limit the level of the out-of-band noise floor. A new and very simple method by which the phase correction circuit is adjusted is described. The scheme uses the supply current to the final stage amplifier as a measure of the out-of-band noise, and minimizes this by using a simple direct search algorithm. Phase correction to within 5 degrees of optimum can be obtained after about 50 iterations.

INTRODUCTION

Feedback is a well known technique for linearising non-linear systems, however if there is a delay in the system , instability can result unless the operational bandwidth is limited. Feedback can be used with non-linear RF power amplifiers by applying it over the modulation bandwidth rather than the full RF bandwidth. This is usually achieved by using a compensation network that takes the form of a bandpass filter or its baseband equivalent (Cartesian feedback) [4, 5, 6,7].

Unfortunately the stability of modulation feedback schemes can be effected by the absolute RF phase shift around the feedback loop which changes with carrier frequency, amplifier device and environmental fluctuations (Vcc, temperature and antenna loading). Incorrect phase adjustment causes the loop phase margin to be reduced. This can cause peaking in the closed loop frequency response near the 0dB gain crossover frequency, which in turn causes an increase in the out-of-band noise floor, 1MHz to 10MHz from the carrier frequency. These phenomena have been experimentally observed in [1] and analyzed in [2]. The adjustment of the loop phase shift is critical for stable operation.

Published methods for controlling the phase adjuster include minimizing the open loop phase difference between the input and feedback signals [1], and using a look-up-table of stored correction values obtained from a special test at manufacture [3]. The former requires the additional overhead of a short test transmission whenever a phase correction is necessary and the latter has difficulty in compensating for device aging or loading variations.

The method described here seeks to adjust the loop phase shift in order to minimize the supply current to the final stage amplifier. The final stage amplifier is usually operated in class C, B or AB for efficiency reasons, in which case the supply current can be used as a measure of the non-linear amplifier's output power. The output power has two components, the desired amplified signal and the undesired out of band noise. Adjustment of the loop phase shifter has little effect on the former but has a large effect on the latter. Minimizing the amplifier output power therefore minimizes the out of band noise and so gives the optimum phase adjustment value.

PHASE and CURRENT

This paper presents measured results from a 50 Watt, 900 MHz class AB amplifier with RF feedback and Cartesian compensation. Figure 1 shows the phase rotator hardware set up, including measurement and control circuits for monitoring the amplifier current. The fundamental building block of this system is a phase adjuster, which is used to change the phase of the carrier (LO) signal. The amount of phase rotation is controlled by a PC through a D/A converter. A digital multimeter is used to measure the voltage across a resistor, which is placed in series with the power line of the amplifier. The GPIB bus provided the necessary interface between the computer and the multimeter. The voltage reading from the multimeter is converted to current (in software) which represents the amplifier's current. The best position for the phase adjuster was found to be in the demodulator arm before the loop filter since this minimizes the out of band noise added to the system by the phase adjuster.

0-7803-3871-5/97/$10.00 © 1997 IEEE

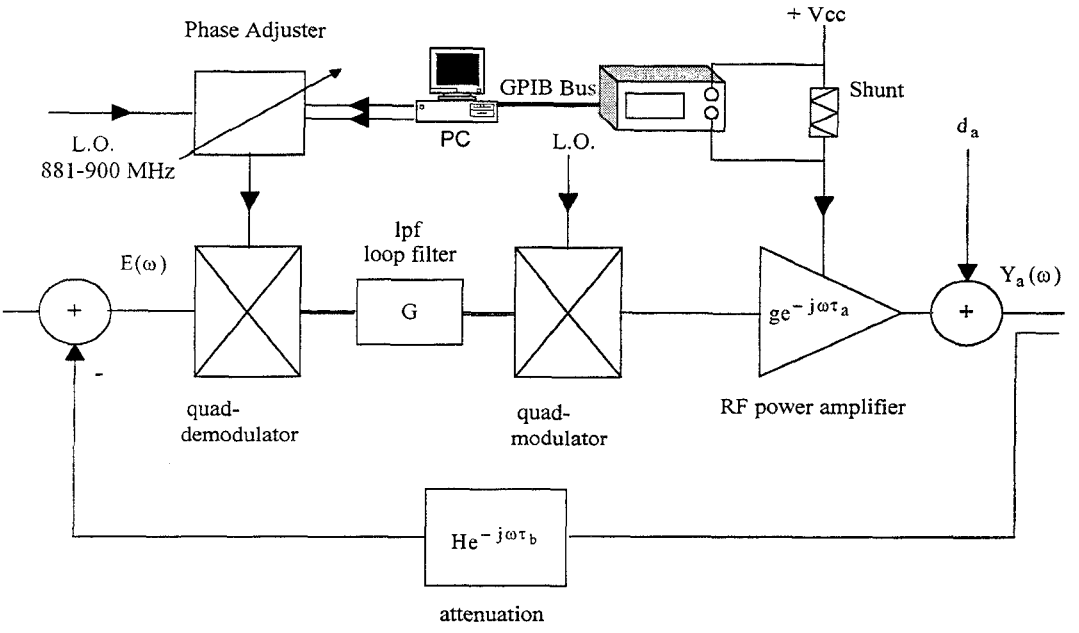

Figure 1 : *Phase rotator experimental set up. Loop gain = 18dB low pass filter bandwidth = 500kHz, loop delay = 36ns [5].*

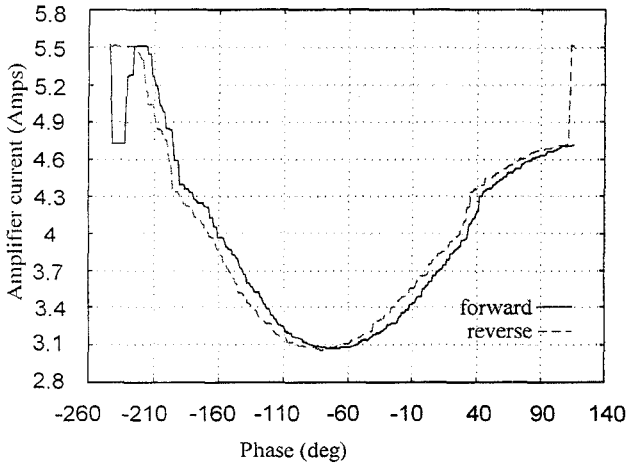

Figure 2: *Amplifier current versus LO phase. Solid trace indicates forward (increasing phase shift) rotation. Dashed trace indicates reverse rotation.*

A plot of the amplifier's current versus phase in shown in figure 2. This plot was obtained from a two-tone test, using a 250 kHz modulation signal centered on 881MHz. The solid curve represents an anti-clockwise (forward) phase rotation through 360^0 , as the system changes from an oscillating state through a stable state, and returns to an oscillating state. The dashed curve represents a clockwise (reverse) phase rotation through 360^0, as the system goes through a similar change of states. The reverse curve appears to be shifted left by ~ 10^0 compared to the forward curve, which means that the amplifier current is sensitive to the direction of phase rotation. For every change in the phase direction, the amplifier current follows a different curve each time. This behavior is described as hysteresis and has important implications on the convergence algorithm. There is a smooth region on both curves where a current minimum is reached that can guarantee stable operation. The current minimizes at the optimum phase adjuster setting of -83^0 and the system is completely unstable at -220^0, with the amplifier operating in the current limit of 5.5 Amps. There is also a sub-optimal minimum near the amplifier saturation region (-240^0), which can be a trap for a one dimensional search algorithm as it searches for a current minimum. Figure 3 shows the hysteresis curves with the input two-tone signal turned off.

On these curves there is a broad minimum which indicates that the amplifier is operating in class AB, since the amplifier current reaches a steady bias level. The phase adjuster cannot be controlled in this zone using the measure of amplifier current. Other techniques must be used in this region. A possible approach is to have the controlling microprocessor set the phase for each carrier frequency using the look-up-table approach [3]. The table is then updated when control over the optimum region is possible. It should be noted that at zero signal levels (or at constant envelope operation) the phase shift through the amplifier is constant and the accuracy of the phase adjuster setting can be reduced by the margin normally taken up by the AM to PM of the amplifier (almost 30^0 in this case).

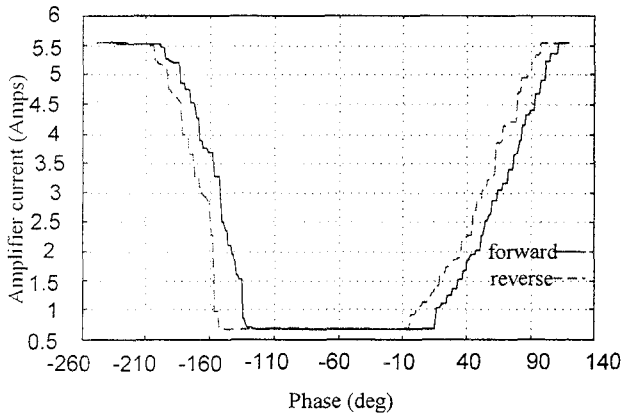

Figure 3: *Hysteresis curves for the no signal condition. Solid curve represents a forward or anticlockwise rotation. Dashed curve represents a reverse rotation.*

ADAPTATION

A simple one-dimensional search algorithm was written first, for the case of a two-tone test. The algorithm aims to minimize the amplifier's current by reading the multimeter from the GPIB interface and adjusting the phase of the LO signal, in steps of $\Delta\phi$ through the phase adjuster. If the current drops after the step $\phi = \phi + \Delta\phi$ has been taken, then the next step is in the same direction, otherwise the direction is reversed. However, any change of phase direction places the new value of current on a different curve because of the hysteresis observed in the current/phase characteristic. The algorithm compares this new value with a value on the previous curve. If the new value is larger the phase is forced to change direction again which makes the next value smaller, since it is found on a lower curve.

The hysteresis can cause the algorithm to drift in the wrong direction and hence the amplifier current grows bigger. This behavior is described by the learning curves in figure 4. The algorithm rapidly minimizes the current but then slows as it hunts for the minimum as expected. However, the amplifier phase continues through the optimum into the oscillation region, as indicated by the current spikes in figure 4. The amplifier is almost in complete instability before the algorithm can re establish control and quickly force the current down again. A closer examination of the current curve shows the existence of two sets of current minima, resulting from the hysteresis found in the amplifier characteristics. The phase also exhibits two sets of optimum values, corresponding to the current minima shown on the current curve.

An improved algorithm was devised to overcome the problem of hysteresis. The phase is only allowed to change direction after three unsuccessful iterations, i.e. iterations where the new value of current is bigger than the old value. This algorithm has run over a long period of time (3000 iterations) and proved to converge to a current minimum with only a small ripple around the optimum point (figure 5). This current ripple corresponds to an increase in out of band noise of about 6dB over the minimum. The step size was 1.4 degrees and the algorithm converged to an optimum phase shift value of 277^0 after 197 iterations. The phase adjustment ripple was 5^0 around the optimum phase shift value and this describes a measure of accuracy of the modified algorithm. Careful study of the current curve shows that the first iteration caused the amplifier to 'snap' into full instability. Convergence was then obtained by the long route. Had the shorter route been established then convergence time would be approximately 3 times faster (83^0 compared to 277^0). The algorithm was modified to always go in one direction if the current limit of the amplifier was exceeded. This stops hunting when the amplifier is in full oscillation.

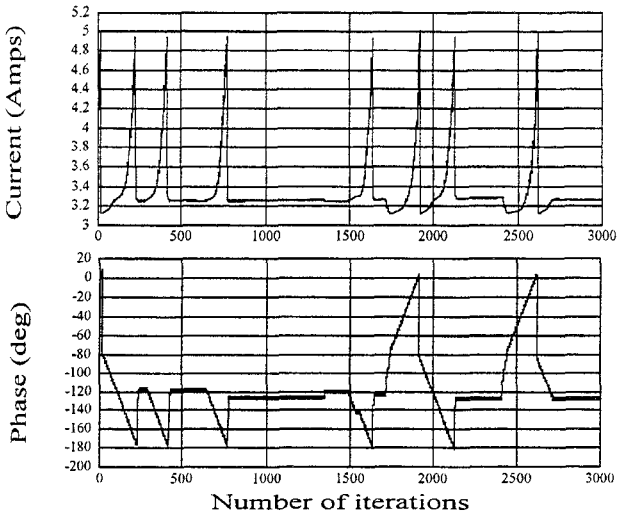

Figure 4: *Amplifier current and loop phase learning curves using a simple one-dimensional search algorithm. Hysteresis in the current / phase characteristics causes drifting.*

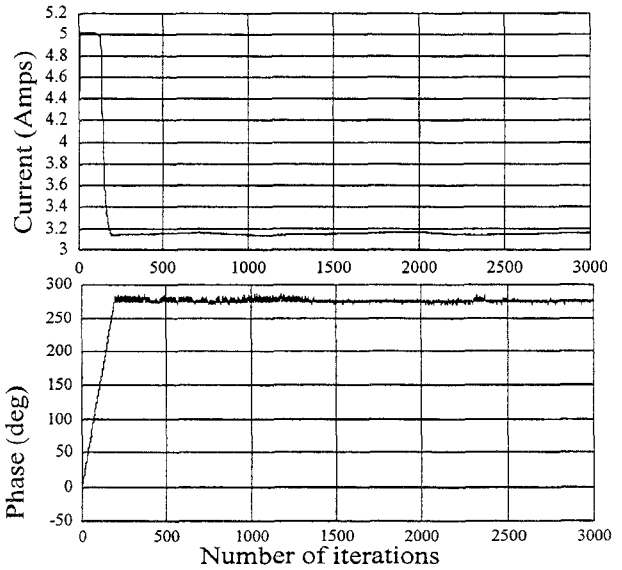

Figure 5: *Amplifier current and loop phase convergence curves using modified algorithm.*

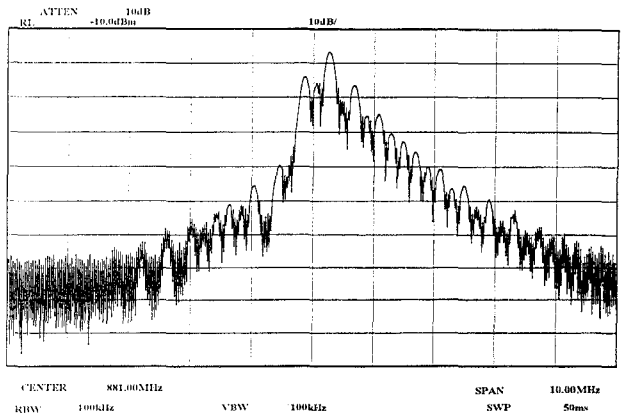

Figure 6: *Amplifier near instability. Spectrum shows increased out of band noise.*

Figure 6 shows the amplifier output spectrum with a phase shift near -180^0, which represents an oscillatory condition. Unwanted spectral components build up to the right side of the center frequency and the system eventually breaks up into sustained oscillation. The amplifier output power rises to a maximum, which corresponds to a current maximum of 5 Amps. The algorithm effectively minimizes the amplifier current and converges to a stable condition, as described by the output spectrum of figure 7.

The improved algorithm was used to test the performance of the system under frequency variations. This experiment was performed for a range of frequencies from 880 MHz to 895 MHz. Figure 8 shows the learning curves for operation under frequency hopping. Starting at 895 MHz, the frequency was gradually dropped to 880 MHz in steps of 1 to 5 MHz and then increased back to 895 MHz. The discontinuities in the current curve indicate sudden changes in frequency for which the algorithm cannot respond instantly.

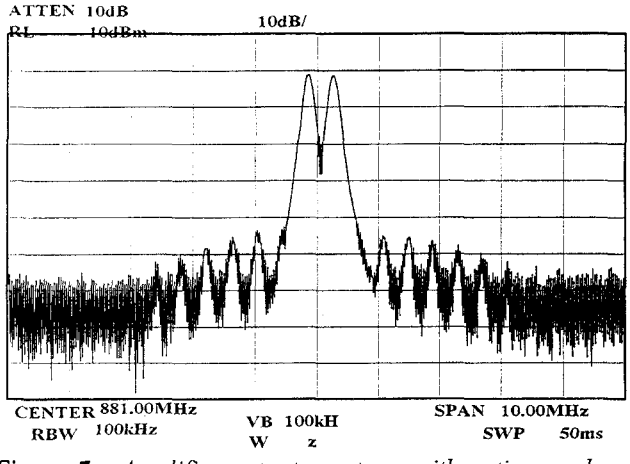

Figure 7: *Amplifier output spectrum with optimum phase adjusted to 277 degrees.*

The response time of the algorithm is described by the current ramps, which indicate a convergence time of less than 50 iterations for frequency changes of less than 5 MHz. The phase ramps correspond to corrections from the optimum phase shift and the ruffled parts indicate phase variations around the optimum phase shift. If the change of frequency is too large the resulting step change in phase can result in amplifier instability which the algorithm takes time to correct from. This can be improved by forcing the algorithm to take larger steps and/or reducing the loop gain to stop spectrum splatter while convergence is taking place.

The actual convergence time depends on the period of each iteration. In this experiment convergence was slow because of the speed limitations of the GPIB instruments. However in a practical situation with random data being transmitted the instantaneous current fluctuates with the signal envelope and this can disturb the algorithm. Either the current must be sampled at the same envelope magnitude or it must be averaged over a number of symbol periods. The former is probably more suitable for narrowband modulations and the latter more suitable for wideband modulations. As an example, if averaging were taken over 50 symbols a system with a baud rate of 200kbaud would converge in about 12.5ms. This is probably fast enough to track changes in antenna loading but not large changes in carrier frequency.

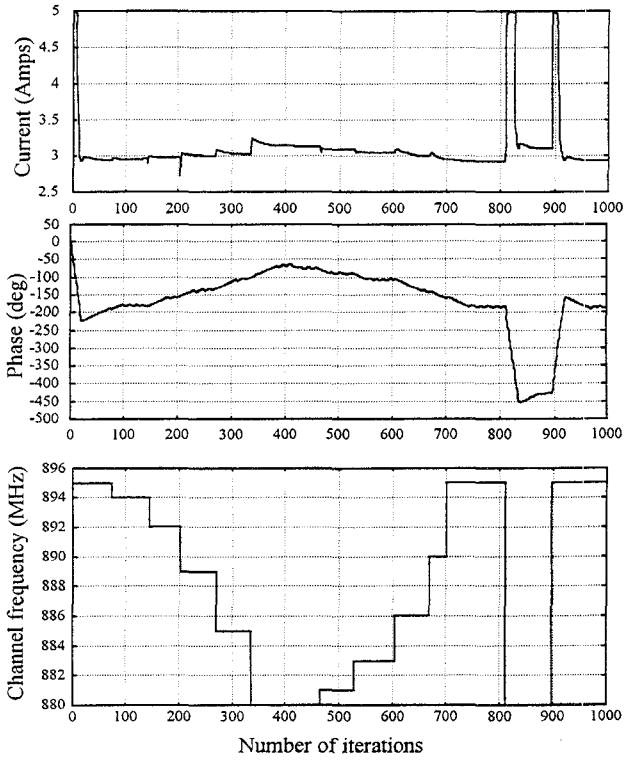

Figure 8: *Convergence behavior of improved algorithm under frequency hopping.*

CONCLUSION

A novel technique for adjusting the RF phase shift in a feedback lineariser was described. The proposed scheme aims to minimize the out of band noise power by monitoring the amplifier current and adjusting the phase accordingly. The main advantages of this scheme are its robustness and simplicity of implementation. It will correct even when the loop is in full oscillation. The disadvantage is its slow initial convergence compared to the symbol rate,

however it appears to be fast enough to track changes in operating conditions such as that caused by antenna load variations. In addition, the scheme will not work for amplifiers in class A operation since the amplifier current does not reflect the output power. This also applies to class AB operation at zero or low output powers. The disadvantages of the scheme can generally be overcome if it is operated as an adjunct to other schemes. For example the table look-up method described in [3]. The look-up table providing fast but coarse correction and the slower scheme described here being responsible for the fine-tuning and table updating.

REFERENCES

[1] Oshima, Y., Minowa, M., Fukuda, E., & Takano, T. (1992). *Cartesian feedback amplifier with soft landing.* In IEEE (Ed.), Int. Symp. Personal Indoor Mobile Radio Commun., (pp. 402-406). IEEE.

[2] Briffa, M., & Faulkner, M. (1996). *Stability analysis of Cartesian feedback linearisation for amplifiers with small nonlinearities.* IEE Proceedings Communications, **143** (4).

[3] Boloorian, M., & McGeehan, J. P. (1995). *Linearisation of frequency hopped transmitters using Cartesian feedback.* In IEEE Vehicular Technology Conference, (pp. 520-524). IEEE.

[4] Ezzeddine, A., Hung, H. A., & Huang, H. (1990). *An MMAC C-band FET feedback power amplifier.* IEEE Trans. Microwave Theory and Techniques, 38 (4), 350-357.

[5] Faulkner, M., Contos, D., & Johansson, M. (1995). *Linearisation of power amplifiers using RF feedback.* IEE Electronics Letters, 31(23), 2023-2024.

[6] Johansson, M., & Mattsson, T. (1991). *Linearised high-efficiency power amplifier for PCN.* Electronics Letters, 27(9), 762-764.

[7] Petrovic, V. (1983). *Reduction of spurious emissions from radio transmitters by means of modulation feedback.* In *IEE Conference on Radio Spectrum conservation techniques*,pp.44-49.

HARDWARE PHOTOS

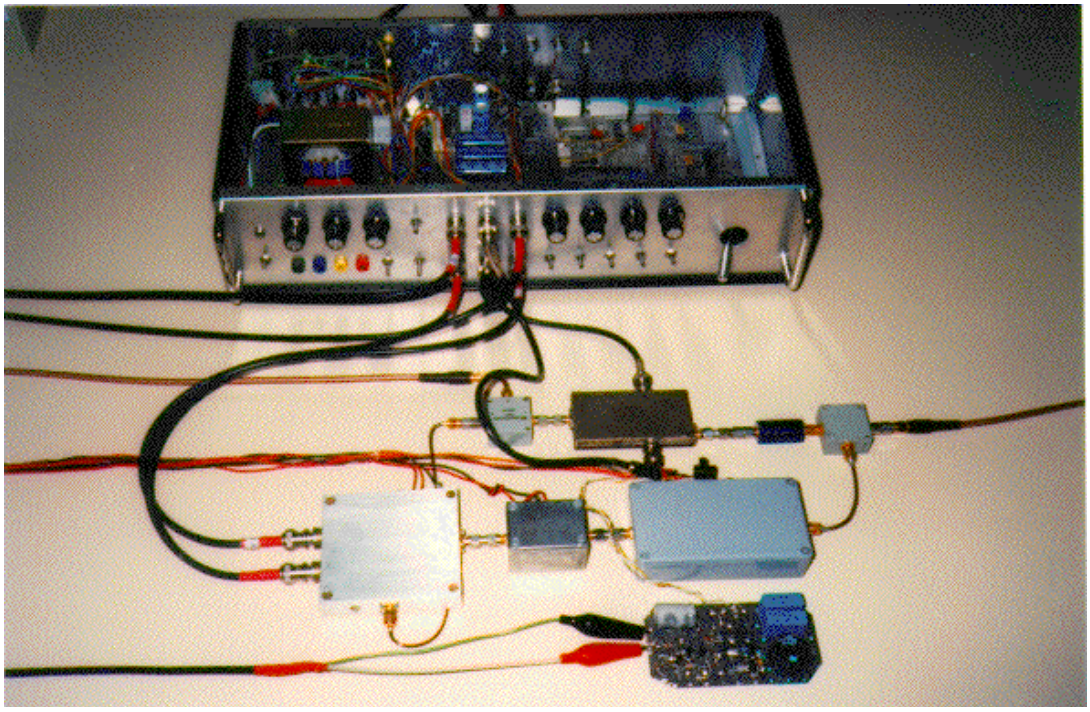

Figure D.1: Cartesian Feedback Box I containing baseband phase rotator and DC offest removal (background), with low power amplifier, and SMPS (foreground).

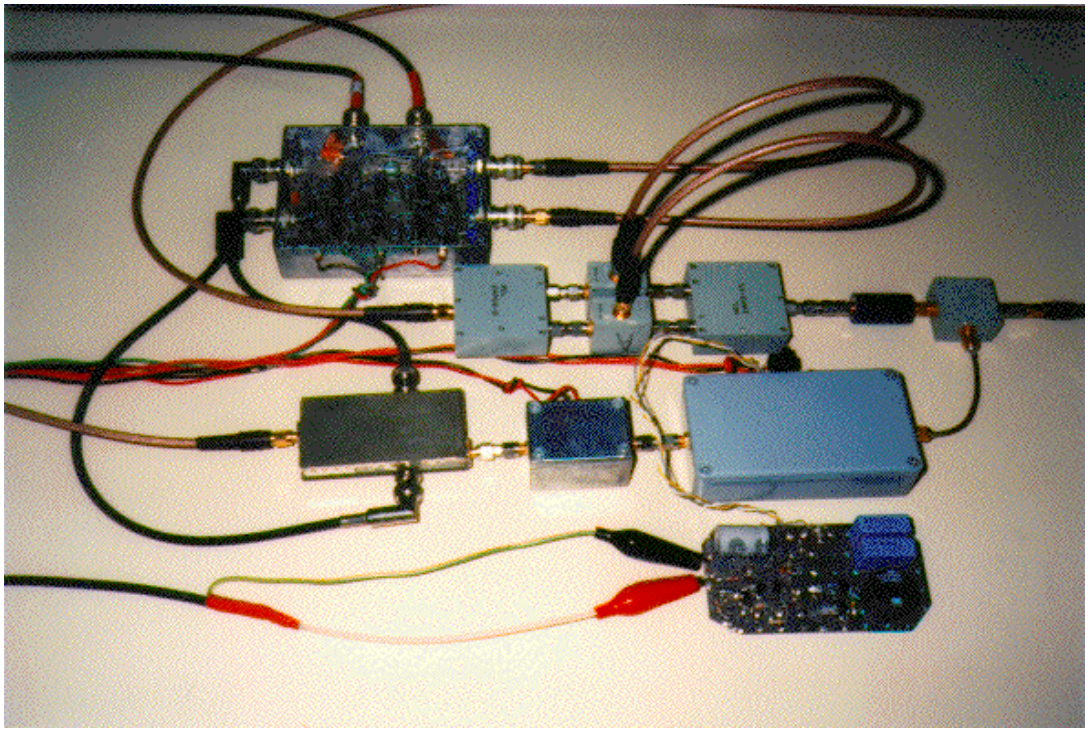

Figure D.2: Cartesian Feedback Box II (background), with low power amplifier, and SMPS (foreground). Results from this set-up was presented in the thesis.

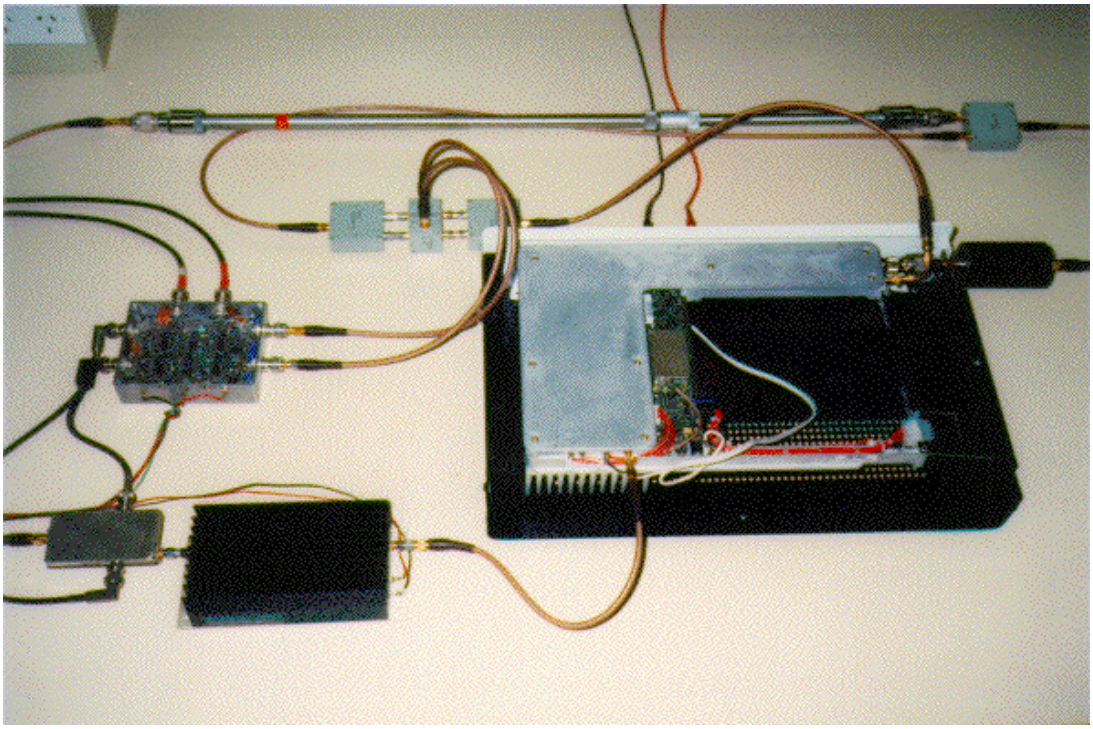

Figure D.3: Cartesian Feedback Box II (left), with line-stretcher (background) and TXPA45 high power amplifier (right). Results from this set-up was presented in the thesis.

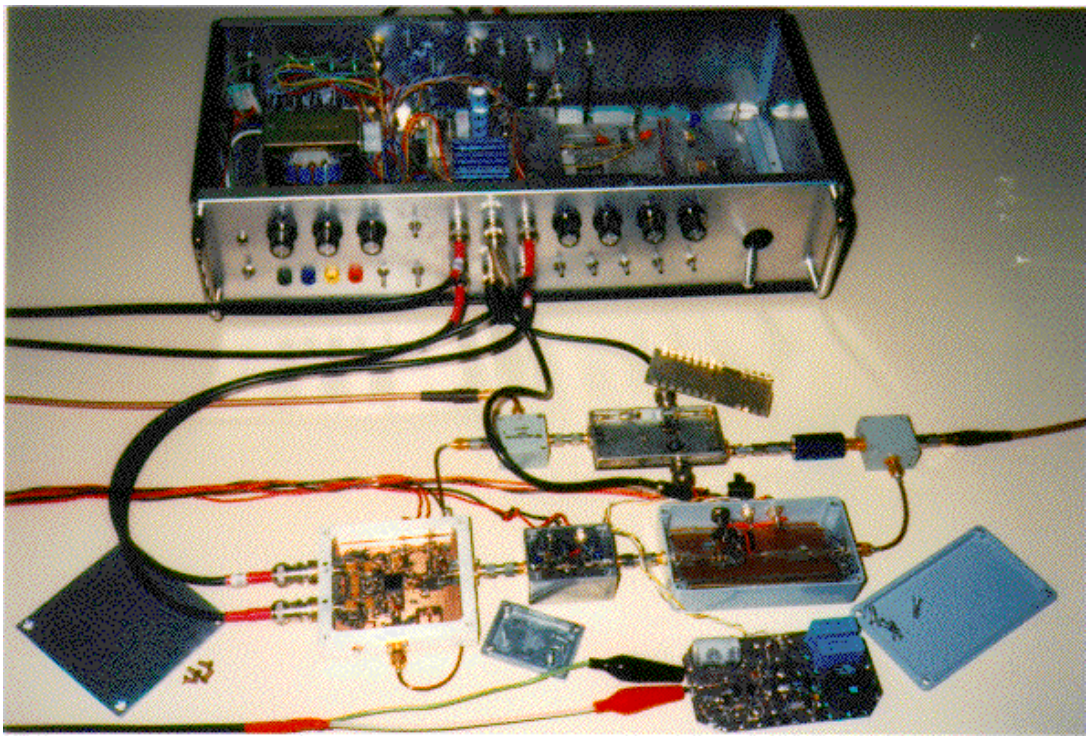

Figure D.4: Cartesian Feedback Box I (background) etc. with lids off.

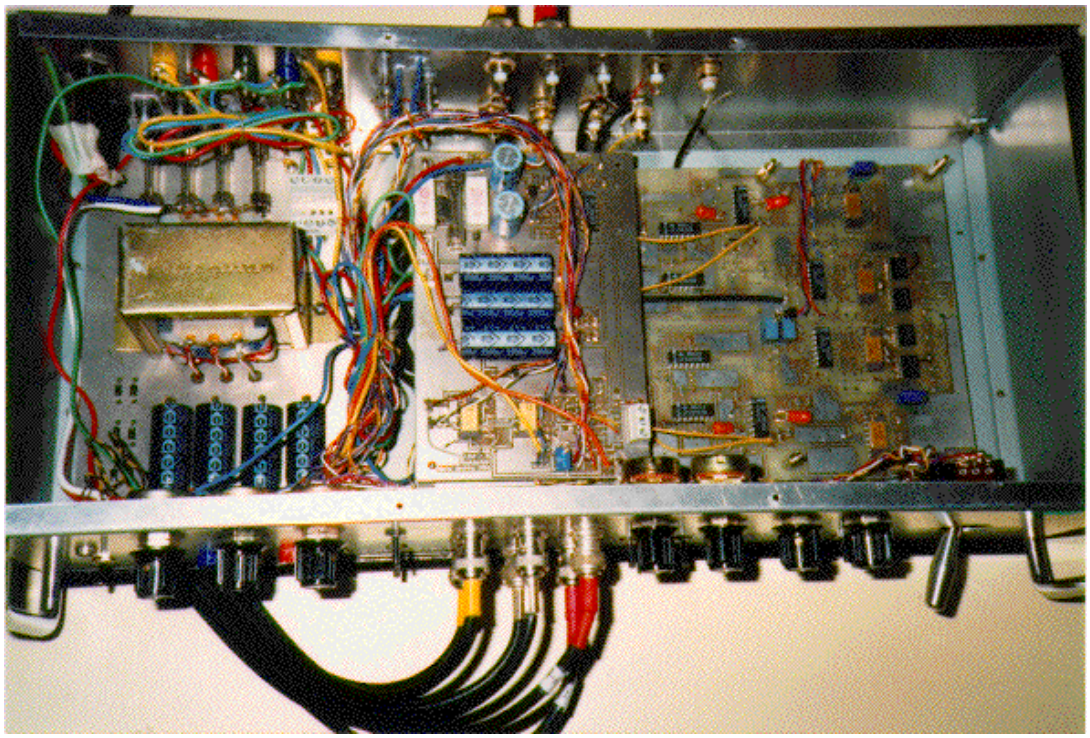

Figure D.5: Cartesian Feedback Box I.

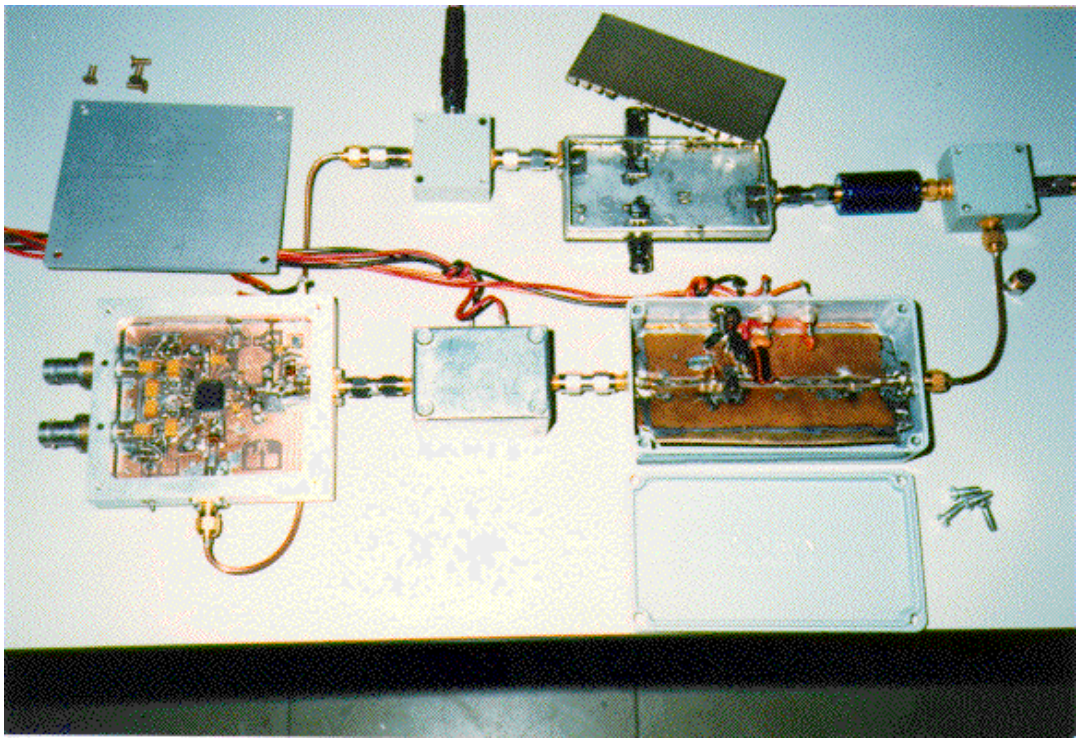

Figure D.6: RF sub-blocks: Active Quadrature Modulator (left), driver(middle), low power PA (right),coupler, low-pass filter and passive Quadrature Demodulator (back).

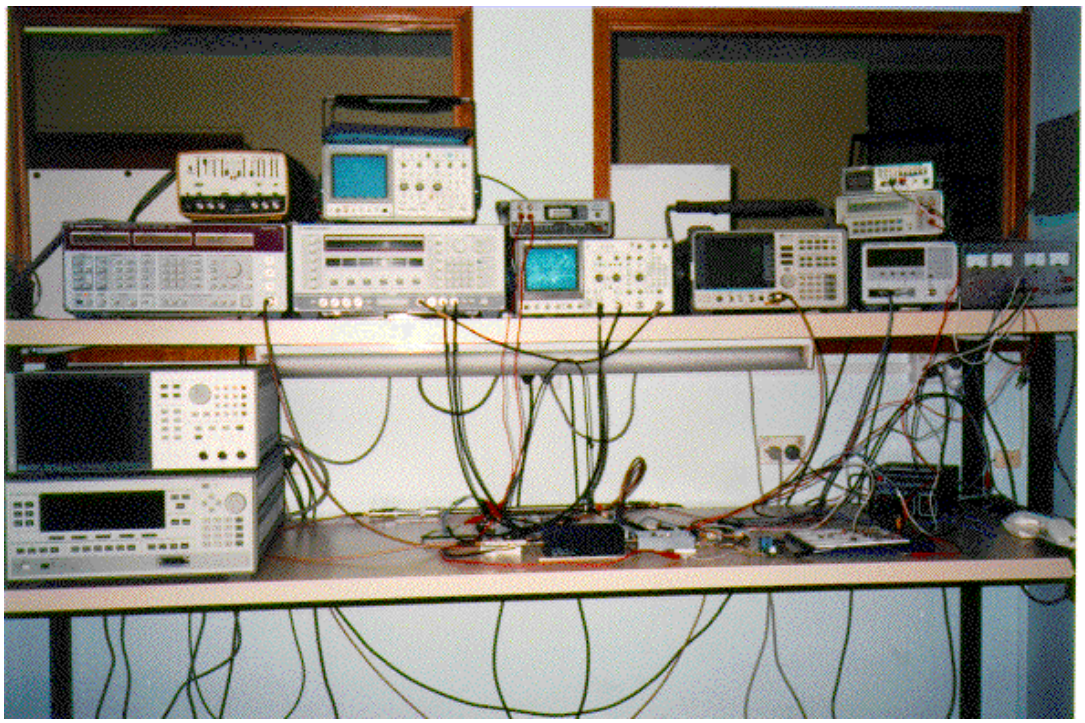

Figure D.7: Lab set-up (lights-on).

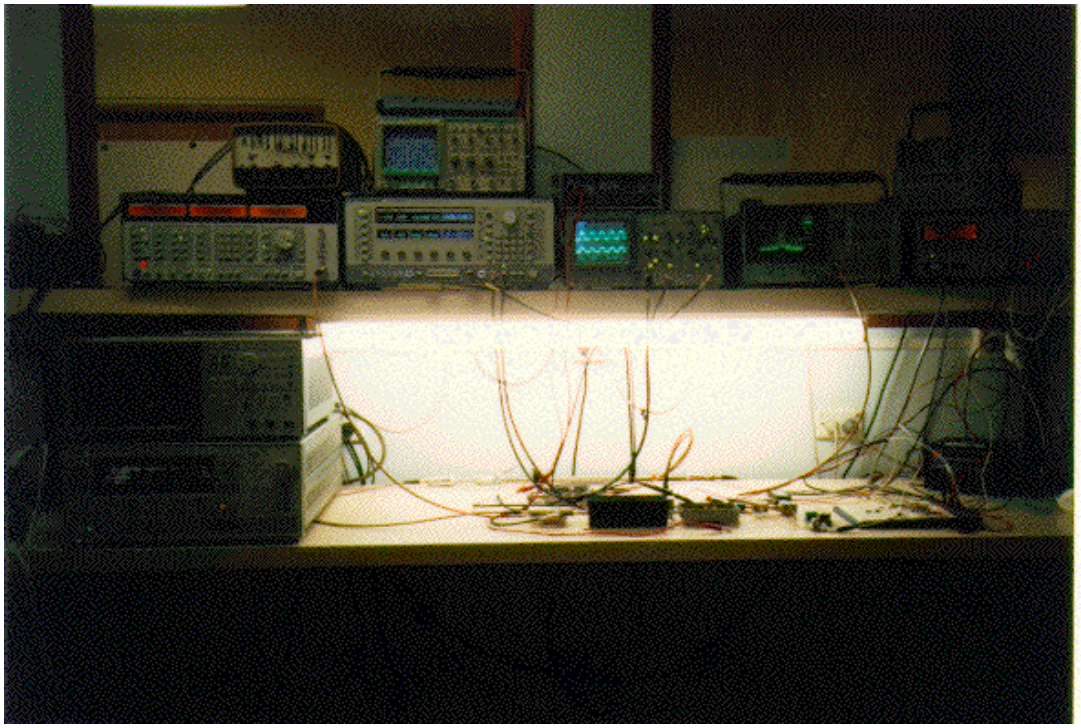

Figure D.8: Lab set-up (lights-off).

Figure D.9: Promo shot in the lab I.

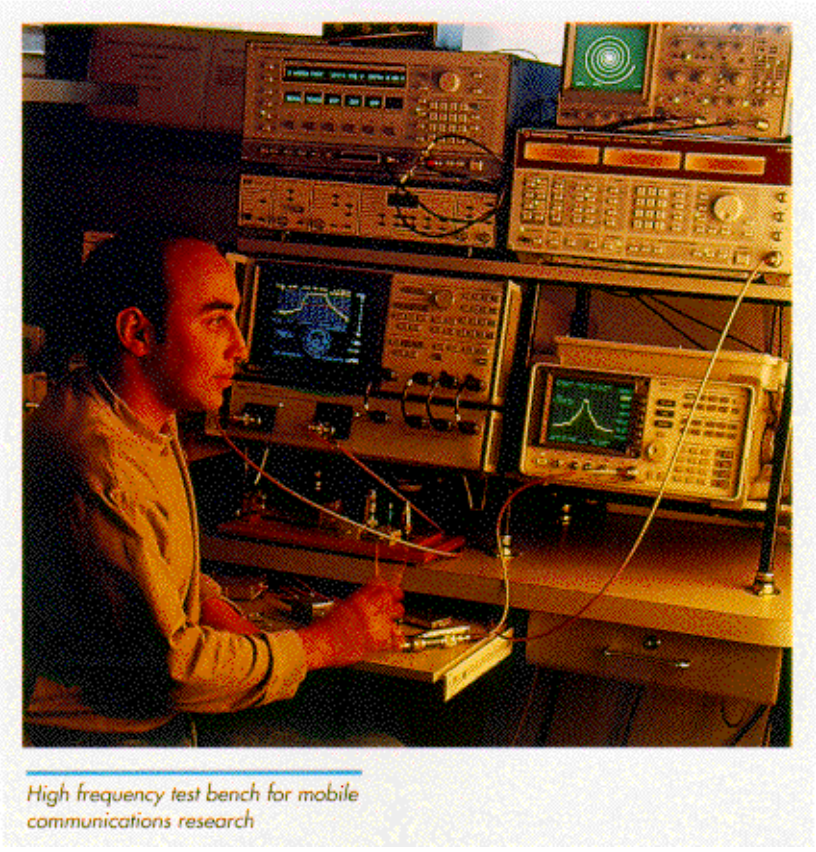

Figure D.10: Promo shot in the lab II.

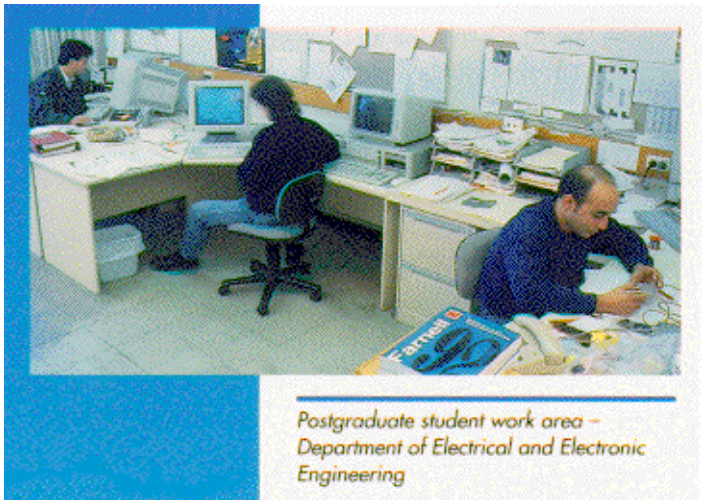

Figure D.11: Promo shot in the office (D720).

UNIVATION

Cartesian Communicators Eye the Prize, Ear the Future

Victoria University of Technology PhD research student, Mark Briffa and supervisor Associate Professor, Mike Faulkner have won the prestigious IERE Benefactors Premium research prize for their work in the field of mobile telecommunications.

The prize, awarded annually by the Institution of Electrical Engineers (IEE) of London, was for a research paper published in the IEE Communications Journal, a major international journal reporting on new technical advances in the field of telecommunications.

The paper, 'Stability analysis of Cartesian Feedback linearisation for amplifiers with weak non-linearities' analyses an important new class of radio frequency amplifier that will be required for the next generation of Mobile Communication equipment.

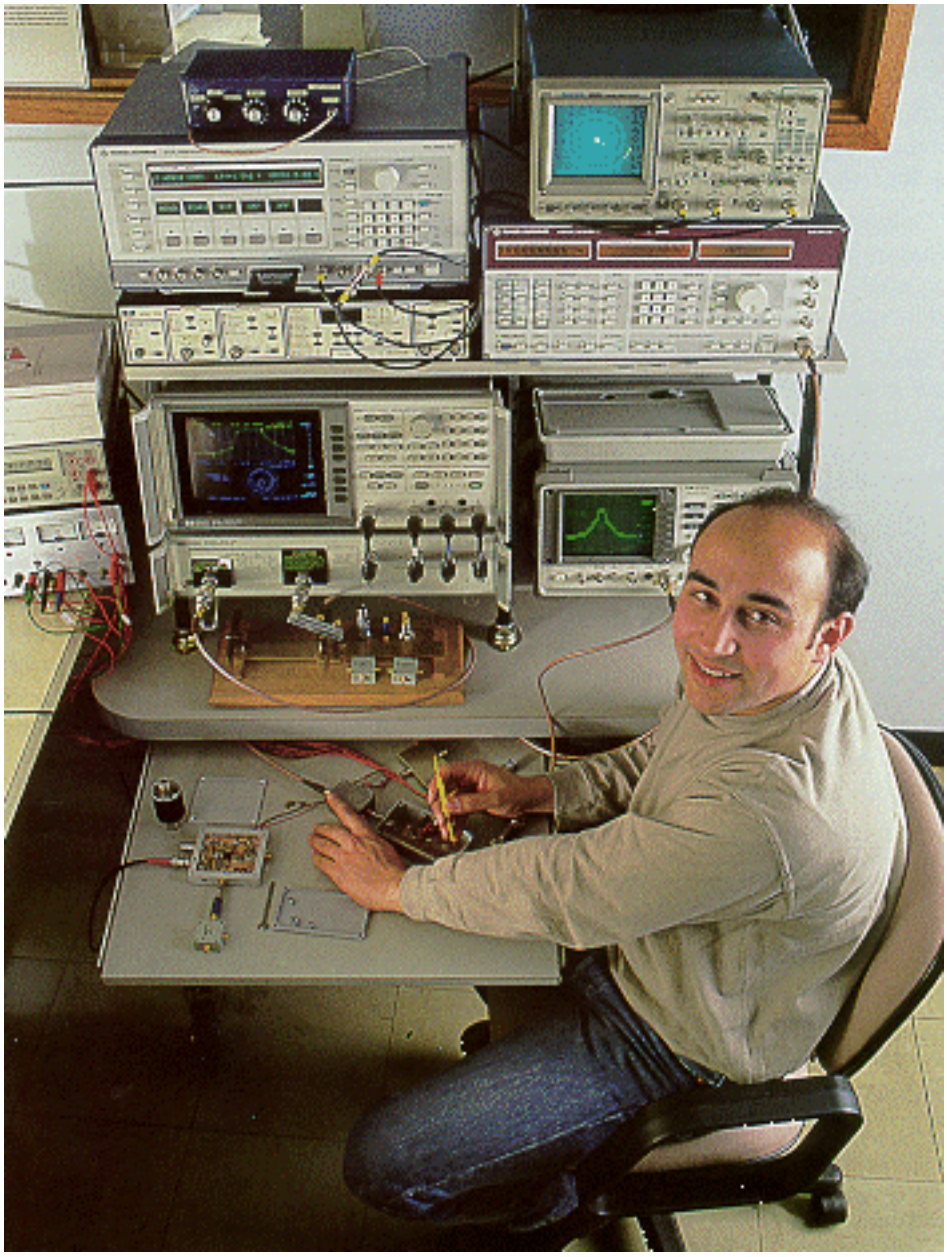

PhD student Mark Briffa.

Associate Professor Faulkner, who leads the Mobile Communications and Signal Processing Group at VUT, said the amplifiers combine high efficiency for long battery life with extreme linearity needed for future radio communications systems.

"This combination has been almost impossible to achieve until now. The amplifiers will be required for new high capacity modulation schemes that improve data throughput by varying both the amplitude and the phase of radio frequency carrier signals."

Associate Professor Faulkner said that current systems in Australia such as the Analog AMPS system and the digital GSM system only vary the phase of the carrier signal.

"Typical applications for linearised amplifiers include the new digital Private Mobile Radio schemes TETRA and APCO originating from Europe and the USA.

"These schemes will be used by private organisations such as taxis companies and emergency services such as the Police and Ambulance. They are likely to be deployed in Australia within the next 12 months and will have up to four times more capacity than existing systems," he said.

Associate Professor Faulkner said the systems are only now being defined and are unlikely to be in service before the year 2002.

"There are also current schemes that are likely to benefit from the amplifiers including the North American and Japanese Digital Cellular Mobile systems and our own Optus Mobiles at system.

"In the future, linearised radio frequency power amplifiers will be used for all future mobile communication systems, so the research results reported in the paper are timely and of direct benefit to industrial companies developing these future products."

For further information contact VUT's Senior Media Officer, on 03 9688 4950 or 014 975 912.

[©] [Univation July 1998 Contents] [Univation Home Page] [AVCC Home Page]

Editorial Contact: Manager, External Relations
Last WWW Update: 21Oct98
WWW Contact: Paul Freeland